ICE SHEET MODELING DURING HIGH-OBLIQUITY CLIMATES ON MARS: APPLICATION TO THARSIS MONTES TROPICAL MOUNTAIN GLACIATION.

J. L. Fastook[1], D. E. Shean[2], J. W. Head[2], and D. R. Marchant[3], [1]Climate Change Institute and Computer Science, Univ. Maine, Orono ME 04469 (fastook@maine.edu), [2]Dept. Geol. Sci., Brown University, Providence RI 02912, [3]Dept. Earth Sci., Boston University, Boston MA 02215.

Introduction: Deposits on the flanks of the large Tharsis Montes volcanoes have been recognized to be of glacial origin [1,2,3]. These Amazonian-aged deposits display three distinct facies, ridged, knobby, and smooth [4], each of which can be associated with different glacial processes [1]. We use the fundamental differences between the atmospheric snow accumulation environments on Earth [5] and Mars [6,7], geological observations [1,2,3,4], and ice sheet models [5,8,9] to show that the Martian ice sheet mass balance can be characterized by two equilibrium lines, and that glacial accumulation is favored on the flanks of large volcanoes, not their summits as seen on Earth. Atmospheric general circulation models for high-obliquity climates show that upwelling and adiabatic cooling of moist polar air will favor deposition of snow on the northwest flanks of the Tharsis Montes [10,11].

Predicted accumulation rates, together with sample spin-axis obliquity histories, are used to show that mean obliquity in excess of 45° and multiple 120 ka obliquity cycles are necessary to produce glaciers and the observed deposits. These results indicate that the formation of these deposits required multiple successive stages of advance and retreat before their full extent could be reached, and thus imply that spin axis obliquity remained at these high values for millions of years during the Late Amazonian. Calculations of precise spin-axis geometry histories prior to about 20 Ma ago are not possible [12,13], but our results provide insight into the nature of the late Amazonian obliquity history of Mars and begin to establish data points for the geologically-based reconstruction of the orbital history of Mars.

Modeling: The ice sheet model used is based on the well-tested shallow-ice approximation [5,8,9]. This combination of mass and momentum conservation yields a partial differential equation for the ice thickness and requires as source the net annual mass balance at each point in the domain. This mass balance distribution is best described with a parameterization, generally in terms of location and elevation, to accommodate an expanding ice sheet that changes elevation, and hence its own climate, as it experiences a cycle of ice-age climate.
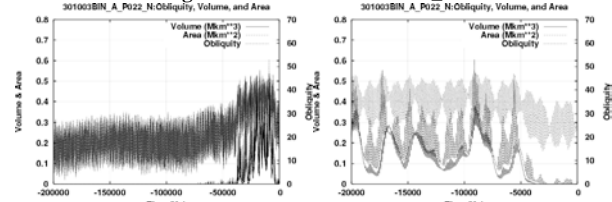
Mass Balance Distribution: In our parameterization, the mass balance consists of two parts, the annual accumulation (ice-equivalent snowfall, in m/yr) and the annual ablation (melting, sublimation, or other erosive processes that remove ice from the ice surface). The difference between these two is the net mass balance, which is the source (or sink if negative) in the shallow-ice equation. The positive accumulation component is generally taken to depend on saturation vapor pressure, which has an exponential dependence on temperature. On Earth the negative ablation component is due to melting, and hence proportional to total Positive Degree Days during an annual cycle of seasons. On Mars it is primarily due to sublimation, which depends on the saturation vapor density (vapor pressure divided by atmospheric pressure) and hence has the same exponential dependence on temperature as the accumulation component of the mass balance. With a vertical lapse rate, reduction of temperature with elevation leads to declining accumulation and sublimation rates. However, with atmospheric pressure in the denominator, sublimation declines less rapidly, leading to overall lower, and possibly negative, net mass balance. Thus on Mars we might expect snow-filled valleys rather than the snow-capped mountains we see on the Earth. Declining relative humidity or increasing ventilation (both of which affect sublimation rates), or some melting at lower elevations will lead to net negative mass balance at low elevation. Thus we will have two equilibrium lines, a high and a low one, with positive mass balance only in between. All of this produces a mass balance distribution that depends on elevation, but the fan-shaped deposits are all on the northwest flanks of the volcanoes. Whatever the cause, the climate parameterization needs some way to produce spatially non-uniform mass balance. Thus we only allow accumulation where the surface slopes within a few degrees of the trend (N62°W) of the Arsia deposit.

Simulations: Climate change on Mars is controlled by orbital variations similar to those thought to cause ice ages on Earth. The primary influence on Mars is thought to be the obliquity, which has much greater variability than on Earth due to the absence of a large moon and its proximity to Jupiter.

Laskar [12,13] has calculated obliquity histories and shown a robust solution for the last 20 Ma. The pattern shows a general 120 ka oscillation with an amplitude of ~10°, within an envelope with a 2 Ma period. Beyond 20 Ma, the solution becomes chaotic (extremely sensitive to initial conditions), but Laskar has published representative obliquity histories back to 250 Ma. We have used these representative scenarios to drive the ice sheet model for the last 200 Ma for the Arsia Mons ice sheet. Since obliquity is not directly connected to the temperature that serves as a "climate knob" in our mass balance parameterization, we have chosen to calibrate this connection by requiring that the maximum areal extent obtained during the 200 Ma simulation match the glacial deposits identified in [1,2,3]. For this reason the calibration for each of the Laskar scenarios will be different, and hence the glaciation response will occur at different times. By comparing with age estimates for the Arsia deposit [14], we hope to be able to distinguish between the different scenarios.

Figures 1-5 show obliquity scenarios calculated by Laskar (P000_N, P001_N, P022_N, N001_N, and N006_N). On each of these are also shown ice volume (lowest dark line) and areal extent (middle grey line) produced by the ice sheet model. In the right-hand figure, the last 20 Ma of each record is shown. The ridged facies is the oldest facies (most likely 100's of Ma [14]), while the innermost deposits around and near the graben at the base of the Arsia shield are most likely to be younger [14]. With this we can rule out scenarios such as P022_N (Figure 1), which only has late ice sheets.

Figure 1: Laskar scenario P022_N.

Scenario P001_N (Figure 2) is also unlikely since the configuration matching the glacial deposits occurs too late. It is worth noting that both P022_N and P001_N, whose full ice configurations occur after 50 Ma, show some limited ice in the graben right up to the present during the low-obliquity phase after 4 Ma.

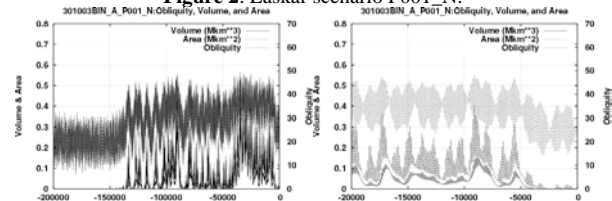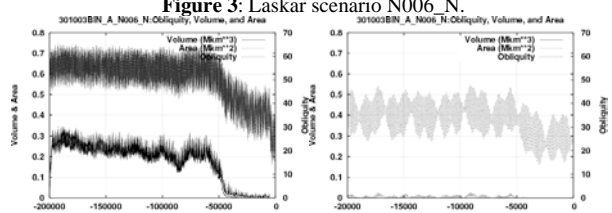**Figure 2**: Laskar scenario P001_N.

Figure 3: Laskar scenario N006_N.

Scenario N006_N (Figure 3) does show large-scale glaciation early in the simulation, but may not have sufficient variation in size to account for the many ridged facies drop moraines. In addition, scenario N006_N does not have significant ice in the Arsia graben post 20 Ma.

Scenarios P000_N and N001_N (Figures 4 and 5) are in best agreement with the crater-count data indicating a late Amazonian age [14]. Both have significant ice sheets before 100 Ma, and both have limited ice compatible with the young deposits in the Arsia graben (no ice after 4 Ma during the low obliquity phase, but some limited ice prior to the shift in levels). The most compelling difference between P000_N and N001_N is that N001_N only shows 4 distinct ice sheet growth events, whereas P000_N has many. Figures 6 and 7 show a magnification of the first 100 Ma for scenarios P000_N and N001_N respectively.

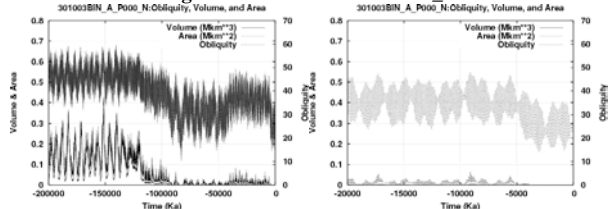**Figure 4:** Laskar scenario P000_N.
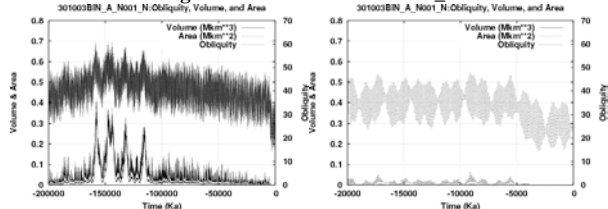

Figure 5: Laskar scenario N001_N.

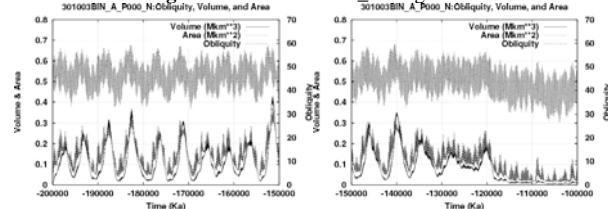**Figure 6:** Scenario P000_N magnified.
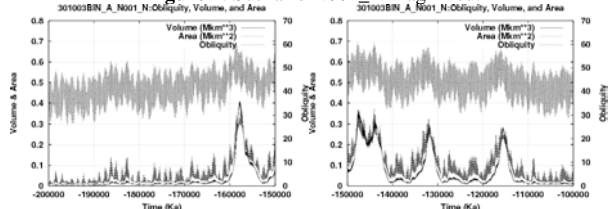

Figure 7: Scenario N001_N magnified.

Figure 8 shows the configuration, thicknesses as colors and surface elevations as contours, for the N001_N peak at 147.5 Ma. This is the configuration used to calibrate the relationship between obliquity and "climate knob," and thus "fits" the glacial deposits, indicated by the dark outline. Also shown in Figure 9 is a typical late configuration (9.1 Ma) that is in accord with relatively young features around the Arsia graben. Accumulation stops in this model after 3.7 Ma ago, when the obliquity has shifted to its lower state. In reality, some buried ice could remain longer [15].

Conclusions: Five scenarios of possible past obliquity histories are used to drive an ice sheet model with a parameterization of climate that allows for variation as the obliquity changes and as the ice sheet grows and shrinks. Two, P022_N and P001_N, are unlikely because they do not agree with age estimates of the ridged facies and have too much late ice. One, N006_N, is unlikely because the areal variability is apparently insufficient to account for the number of drop moraines

in the ridged facies. Two, P000_N and N001_N, are plausible, both in the timing of the maximum configurations and in the limited configuration of ice during the very recent past [14]. Further analysis will help to establish a geologically-based reconstruction of the orbital history of Mars.
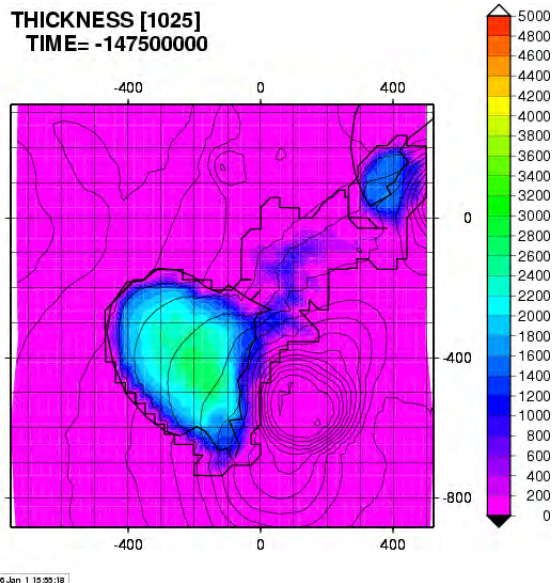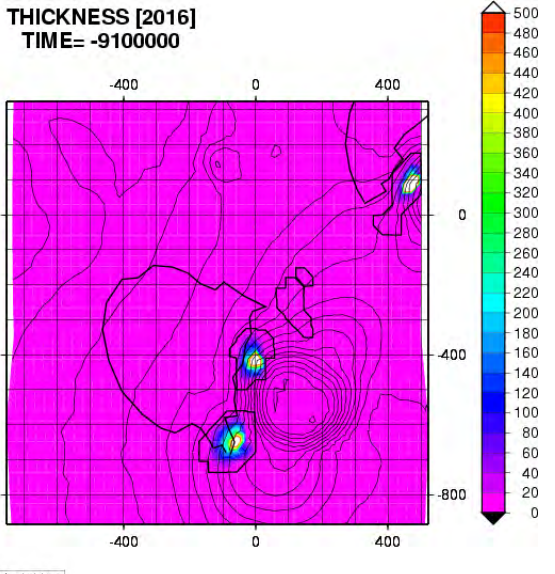
Figure 8: N001_N at 147.5Ma peak configuration.

Figure 9: N001_N at 9.1 Ma late configuration.

References:
[1] Head J. and Marchant D. (2003) *Geology*, 31, 641-644. [2] Shean D. et al. (2005) *JGR*, 108, doi:10.1029/2004JE002360. [3] Shean D. et al. (2004) *LPSC 35*, #1428. [4] Scott D. and Zimbelman J. (1995) Map I-2480, *USGS Misc. Invest. Ser.* [5] Fastook J. and Prentice M. (1994) *J. Glaciology*, 40, 167-175. [6] Fastook J. et al. (2004) *LPSC 35*, #1452. [7] Fastook J. et al. (2005) *LPSC 36*, #1212. [8] Fastook J. (1993) *Computational Science and Engineering*, 1, 55-67. [9] Huybrechts P. et al. (1996) *Ann. Glaciology*, 23, 1-12. [10] Haberle R. M. et al. (2004) *LPSC 35*, #1711. [11] Forget F. et al. (2005) *Science*, in press. [12] Laskar J. et al. (2004) *Icarus*, 170, 343-364. [13] Laskar J. et al. (2004) *LPSC 35*, #1600. [14] Shean D. et al. (2006) *LPSC 37*. [15] J. Helbert et al., *LPSC 37*, #1371, 2006.